Design of a static anti-windup compensator which guarantees robust stability[§]

Nobutaka Wada[†,‡], Masami Saeki[†]

***Abstract*— In this paper, a design method of a static anti-windup compensator which guarantees robust stability subject to saturation nonlinearities and which attenuates a windup phenomena is proposed. Although this design problem has been considered as a non-convex problem in the previous works, we will show that it can be converted into a convex optimization problem with linear matrix inequality constraints. Three numerical examples show effectiveness of the proposed method.**

I. Introduction

In many practical control systems, there exist saturation limitations on controller outputs. It is well-known that input saturations give adverse effects on control performance called windup phenomena [13]. An anti-windup scheme is one way to deal with the windup phenomena and is usually performed by adding an anti-windup compensator to the controller which gives acceptable performance in the unsaturated region [8], [4], [2], [3]. Recently, several design methods of an anti-windup compensator which considers closed-loop stability have been presented. In [2], [3], this design problem is reduced to a BMI problem, and an alternating minimization algorithm is applied to solve it. However, a global optimal solution cannot be obtained by this algorithm in general [10].

In this paper, we propose a design method of an anti-windup compensator which guarantees closed-loop stability. Firstly, we derive a robust stability condition of the anti-windup control system based on the multivariable circle theorem, and show that this condition can be converted into a LMI condition. Secondly, we derive a condition which the control system should satisfy to attenuate the performance degradation during saturation period. Then, we formulate the design problem of an anti-windup compensator which satisfies both the robust stability condition and the performance condition in the Multi-Objective design framework of the LMI method. Finally, the proposed design method is applied to three numerical examples.

II. Problem Statement

Consider a feedback control system shown in Fig.1. $P(s)$ and $K(s)$ represent a plant and a controller respectively, and

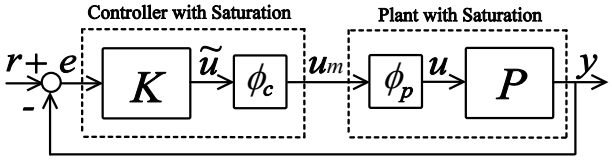

Fig. 1. Actual control system

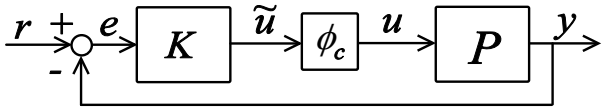

Fig. 2. Equivalent control system

their state equations are given by

$$P: \left\{ \begin{array}{lcl} \dot{x}_p &=& A_p x_p + B_p u \\ y &=& C_p x_p \end{array} \right. \tag{1}$$

$$K: \left\{ \begin{array}{lcl} \dot{x}_c &=& A x_c + B e \\ \tilde{u} &=& C x_c + D e \end{array} \right. \tag{2}$$

where $x_p \in \mathcal{R}^{n_p}, x_c \in \mathcal{R}^{n_c}, u \in \mathcal{R}^p$ and $y \in \mathcal{R}^q$. ϕ_p denotes an actual input saturation, and ϕ_c denotes a saturation function inserted to protect a plant. We make the following assumptions.

Assumption 1: The controller $K(s)$ has been already designed so that the control system has acceptable performance in the unsaturated region.

Assumption 2: The saturation function ϕ_c is chosen so that $u_m = u$ hols for all time.

When the assumption 2 holds, we can disregard the actual input saturation ϕ_p. Hence, in the following we will consider the system shown in Fig.2.

We define the saturation function ϕ_c as

$$\phi_c(\tilde{u}) = (\phi_{c1}(\tilde{u}_1), \cdots, \phi_{cp}(\tilde{u}_p))^T \tag{3}$$

where

$$\phi_{ci}(\tilde{u}_i) = \left\{ \begin{array}{ll} u_{imax} & (\tilde{u}_i > u_{imax}) \\ \tilde{u}_i & (u_{imin} \le \tilde{u}_i \le u_{imax}) \\ u_{imin} & (\tilde{u}_i < u_{imin}) \end{array} \right.$$

Then, we introduce the anti-windup controller $\tilde{K}(s)$.

$$\tilde{K}: \left\{ \begin{array}{lcl} \dot{x}_c &=& A x_c + B e + H(u - \tilde{u}) \\ \tilde{u} &=& C x_c + D e \end{array} \right. \tag{4}$$

$H \in \mathcal{R}^{n_c \times p}$ is a constant matrix, and we refer to it as a static anti-windup compensator. Since we have assumed

[§] The original version of this manuscript (in Japanese) has been published in *Transaction of the Institute of Systems, Control and Information Engineers*, Vol.12, No.11, pp.664/670 (1999)

[†]Dept. of Mechanical System Engineering, Hiroshima University, 1-4-1 Kagamiyama, Higashi-Hiroshima, 739-8527 JAPAN

[‡]Corresponding author. nwada@hiroshima-u.ac.jp

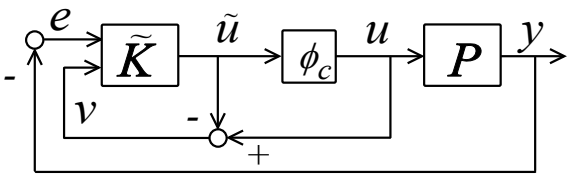

Fig. 3. Control system with an anti-windup controller

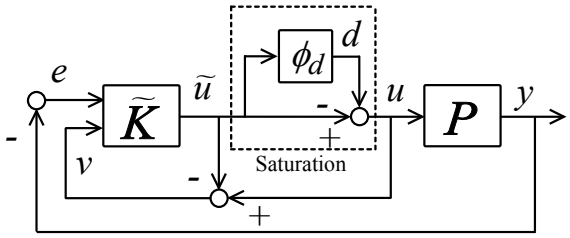

Fig. 4. Control system with a dead zone nonlinearity

that the matrices A, B, C and D are given, the matrix H is the only design parameter. In the following discussion, we will consider the design problem of H which satisfies the following design specifications.

- To stabilize the closed-loop system shown in Fig.3
- To attenuate the performance degradation in the saturated region

III. Design Method

A. Robust Stability Condition

In this section, we derive a robust stability condition of the system in Fig.3, and show that the design problem of the matrix H which satisfies this condition can be reduced to an equivalent LMI problem.

By introducing a dead zone function $\phi_d(\cdot)$, the saturation function $\phi_c(\cdot)$ can be expressed as

$$\phi_c(\tilde{u}) = \tilde{u} - \phi_d(\tilde{u}) \tag{5}$$

where

$$\phi_d(\tilde{u}) = (\phi_{d1}(\tilde{u}_1), \cdots, \phi_{dp}(\tilde{u}_p))^T$$

It can be shown that the closed-loop system of Fig.3 can be transformed into the system of Fig.4 by using (5). Next, as shown in Fig.5, we model the dead zone function $\phi_{di}(\cdot)$ as the sector bounded nonlinearity which lies inside the sector $[0, \bar{\kappa}_i]$. Obviously, the sector entirely covers $\psi_i(\cdot)$ for $\bar{\kappa}_i = 1$ and covers the finite region with the center $\tilde{u}_i = 0$ for $0 < \bar{\kappa}_i < 1$. By using this model, the closed-loop system in Fig.4 can be expressed as the system in Fig.6, where $\Delta_d = \mathrm{diag}(\Delta_{d1}, \cdots, \Delta_{dp})$, $\Delta_{di} \in [0, 1] \quad \forall i$, $\bar{\kappa} = \mathrm{diag}(\bar{\kappa}_1, \cdots, \bar{\kappa}_p)$. Moreover, $\tilde{G}(s)$ is defined by

$$\begin{aligned} \tilde{G}(s) &= \left[\begin{array}{cc|c} A & -BC_p & H \\ B_pC & A_p - B_pDC_p & B_p \\ \hline C & -DC_p & 0 \end{array}\right] \\ &=: \left[\begin{array}{c|c} \tilde{A} & \tilde{B} \\ \hline \tilde{C} & 0 \end{array}\right] \end{aligned} \tag{6}$$

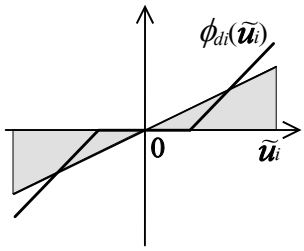

Fig. 5. Deadzone nonlinearity

From the multivariable circle theorem [11], if the following condition holds,

$$(\bar{\kappa}\tilde{G}(j\omega) + I) + (\bar{\kappa}\tilde{G}(j\omega) + I)^* > 0, \quad \forall\omega \tag{7}$$

Then the closed-loop system shown in Fig.6 is asymptotically stable in a neighborhood of the origin.

By applying the following lemma, the condition (7) can be reduced to an LMI condition.

Lemma 1 (The Strictly Positive Real condition [9]): For a given stable transfer function $G(s) := C(sI - A)^{-1}B + D$, the following statements are equivalent.

1) $G(s)$ is strictly positive real.
2) $\exists X = X^T > 0$ such that

$$\left[\begin{array}{cc} XA^T + AX & B - XC^T \\ B^T - CX & -(D + D^T) \end{array}\right] < 0$$

From Lemma 1, the condition (7) holds if and only if there exist $X_S = X_S^T > 0$ and H such that

$$F_S(X_S, H) := \left[\begin{array}{cc} X_S\tilde{A}^T + \tilde{A}X_S & \tilde{B} - X_S\tilde{C}^T\bar{\kappa} \\ \tilde{B}^T - \bar{\kappa}\tilde{C}X_S & -2I \end{array}\right] < 0 \tag{8}$$

Note that the condition (8) is an LMI with respect to H and X_S, since only $\tilde{B}$ includes H.

Remark 1: We explain the reason why the matrix H does not appear in $\tilde{A}$ and only appears in $\tilde{B}$. From eq.(5), the following relation can be obtained.

$$\begin{aligned} v &= u - \tilde{u} \\ &= (\tilde{u} - d) - \tilde{u} \\ &= -d \end{aligned} \tag{9}$$

where $d = \psi(\tilde{u})$. Thus, as shown in Fig.7, the local feedback loop from $\tilde{u}$ to the controller via v can be deleted by using the sector transformation (5). This implies that only $\tilde{B}$ includes H.

Remark 2: In previous studies, the design problem of the matrix H which guarantees the closed-loop stability has been considered a BMI problem [2], [3], [6]. For example, in [2], the robust stability condition is derived as follows. Let $M(s)$ be a transfer function matrix from u to $\tilde{u}$ of the system in Fig.3 with $\Phi = 0$. From the circle theorem, another robust stability condition of this closed-loop system is derived as

$$(-M(j\omega) + I) + (-M(j\omega) + I)^* > 0, \quad \forall\omega \tag{10}$$

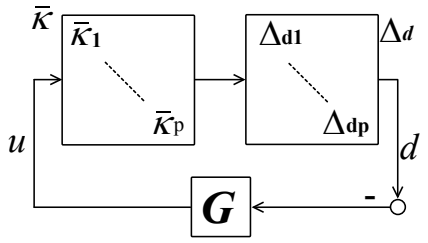

Fig. 6. Closed-loop system for circle theorem

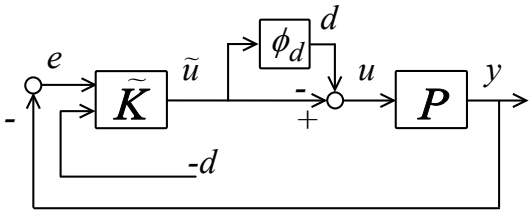

Fig. 7. Disturbance feedforward

where

$$M(s) = \left[\begin{array}{cc|c} A-HC & (HD-B)C_p & H \\ 0 & A_p & B_p \\ \hline C & -DC_p & 0 \end{array}\right]$$

When we apply Lemma 1 to the condition (10), the derived matrix inequality condition has bilinear terms with respect to H and X. Hence the design problem becomes a BMI problem. From the same reason, the design problem of [6] is reduced to a BMI problem.

B. Control Performance Condition

In this section, we consider a condition which the matrix H should satisfy to attenuate performance degradation during saturation period. If we consider the effects of the input saturation as the fictitious disturbance d, it is expected that the performance degradation can be attenuated by making a transfer function from d to y small. Thus we use the following condition as the control performance condition during the saturation period.

$$\|T_{yd}\|_\infty < \epsilon \tag{11}$$

where

$$T_{yd}(s) = \left[\begin{array}{c|c} \tilde{A} & \tilde{B} \\ \hline C_y & 0 \end{array}\right], \quad C_y = \left[\begin{array}{cc} 0 & -C_p \end{array}\right]$$

$T_{yd}(s)$ denotes the transfer function from d to y of the closed-loop system shown in Fig.4 with $\psi = 0$. We use the H_∞ norm to measure the size of the transfer function in the condition (11), since the property of the signal d is unclear in general. By applying the following lemme, the condition (11) can be reduced to an equivalent LMI condition.

Lemma 2 (The bounded-real lemma [9]): For a given stable transfer function $G(s) := C(sI - A)^{-1}B + D$, the following statements are equivalent.

1) $\|G(s)\|_\infty < \gamma$
2) There exist $X = X^T > 0$such that

$$\left[\begin{array}{ccc} AX + XA^T & XC^T & B \\ CX & -\gamma I & D \\ B^T & D^T & -\gamma I \end{array}\right] < 0 \tag{12}$$

From Lemma 2, the condition (11) holds if and only if there exist $X_N = X_N^T > 0$ and H such that

$$F_N(X_N, H) := \left[\begin{array}{ccc} \tilde{A}X_N + X_N\tilde{A}^T & X_N C_y^T & \tilde{B} \\ C_y X_N & -\epsilon I & 0 \\ \tilde{B}^T & 0 & -\epsilon I \end{array}\right] < 0 \tag{13}$$

The condition (13) is an LMI with respect to H and X_N, since only $\tilde{B}$ includes H.

C. Design Problem

We formulate the design problem of H that satisfies conditions (8) and (13) as follows.

Problem 1: Find the matrix H such that

$$\left[\begin{array}{cc} F_N(X_N, H) & 0 \\ 0 & F_S(X_S, H) \end{array}\right] < 0$$
$$X_N = X_N^T > 0$$
$$X_S = X_S^T > 0$$

Note that the above problem is an LMI problem with respect to X_N, X_S and H. Thus Problem 1 is the LMI problem and it can be solved efficiently by using the interior point algorithm [12]. We need to choose $\bar{\kappa}$ to solve Problem 1. Clearly, if Problem 1 is solvable with $\bar{\kappa} = I$, the global stability can be assured by using the obtained anti-windup compensator. However, Problem 1 is not always solvable with $\bar{\kappa} = I$. In such a case, $\bar{\kappa}$ should be chosen as large as possible, since the region of attraction tends to be larger by choosing larger $\bar{\kappa}$.

In addition, it should be noted that we can put any linear structural constraint on the matrix H. A typical and useful constraint is a diagonal structure on H. This constraint can be used for the design of the decentralized anti-windup compensator for the decentralized controller.

IV. Numerical Examples

A. Example 1 (SISO Plant Case)

Let us consider a plant $P(s)$ and a controller $K(s)$ given by

Plant $P(s)$:

$$A_p = \left[\begin{array}{cc} -0.01 & 1 \\ 0 & -0.01 \end{array}\right], B_p = \left[\begin{array}{c} 0 \\ 1 \end{array}\right], C_p = \left[\begin{array}{cc} 1 & 0 \end{array}\right]$$

Controller $K(s)$:

$$A = \left[\begin{array}{cccc} 0 & 1.000 & -2.414 & 2.414 \\ -2.414 & -2.414 & -2.000 & 1.000 \\ 1.000 & 0 & -2.414 & 2.414 \\ 0 & 0 & 0 & 0 \end{array}\right], B = \left[\begin{array}{c} 0 \\ 0 \\ 0 \\ 1 \end{array}\right]$$
$$C = \left[\begin{array}{cccc} 2.414 & 2.414 & 1.000 & 0 \end{array}\right], D = 0$$

A controller output is constrained between the saturation limits ± 0.1.

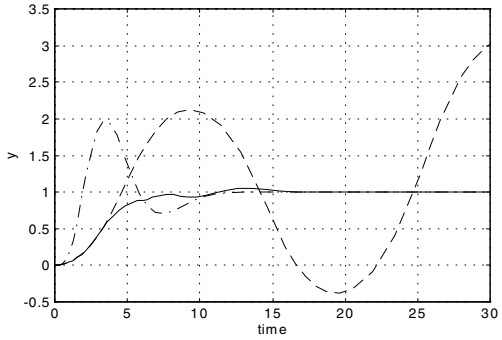

Fig. 8. $y(t)$ (solid:with AWC, dash-dot:unconstrained, dashed:constrained w/o AWC)

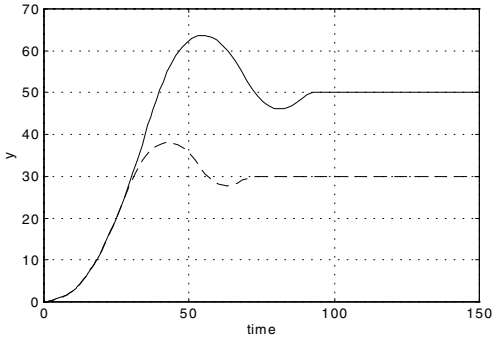

Fig. 10. $y(t)$ (solid:$r(t) = 50, (t \geq 0)$, dashed:$r(t) = 30, (t \geq 0)$)

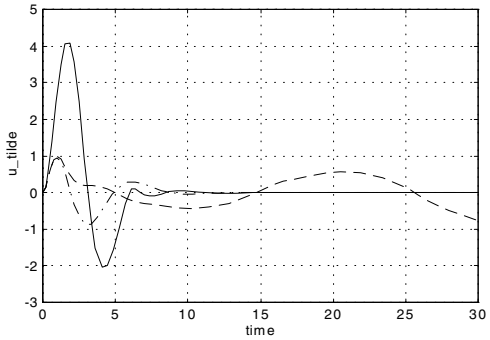

Fig. 9. $\tilde{u}(t)$ (solid:with AWC, dash-dot:unconstrained, dashed:constrained w/o AWC)

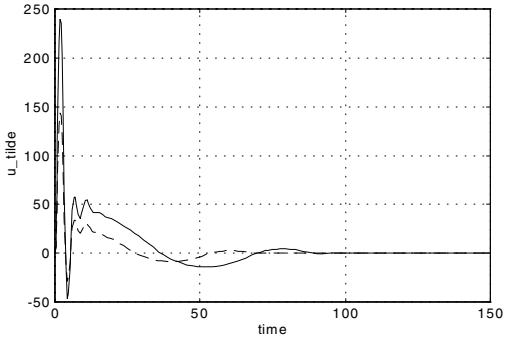

Fig. 11. $\tilde{u}(t)$ (solid:$r(t) = 50, (t \geq 0)$, dashed:$r(t) = 30, (t \geq 0)$)

We solved Problem 1 with $\epsilon = 1.2$ and $\bar{\kappa} = 0.9$, and obtained a feasible solution

$$H = \begin{bmatrix} -0.3823 \\ -1.2552 \\ 0.6082 \\ 0.9837 \end{bmatrix}$$

We chose $\bar{\kappa} = 0.9$, since Problem 1 is not solvable for $\bar{\kappa} = 1$.

Fig.8 and Fig.9 show the responses of the system for $r(t) = 1, (t \geq 0)$. Although the constrained system without the anti-windup compensator becomes unstable (dashed), the closed-loop stability is assured by using the proposed anti-windup compensator (solid).

Since the anti-windup compensator is designed with $\bar{\kappa} = 0.9$, the global stability can not be assured by using this anti-windup compensator. Thus we will check the largeness of the region of attraction by applying large reference commands. Fig.10 and Fig.11 show the responses of the system for $r(t) = 30, (0 \leq t)$ and $r(t) = 50, (0 \leq t)$. In both cases, the system is stable, and the controlled output $y(t)$ tracks the reference command. From these results, we can expect that the region of attraction is considerably expanded by using the proposed anti-windup compensator.

Fig.12 and Fig.13 show the responses of the system with the anti-windup compensator designed with several different ϵ. From these figures, we can see the tendency that the response of $y(t)$ becomes faster in the case where ϵ is chosen to be small. However, the response of $y(t)$ slightly oscillates when $\epsilon = 0.7$. Thus we should choose a smaller value as ϵ unless the system oscillates.

B. Example 2 (MIMO Plant Case)

Let us consider the example of [8]. The coefficient matrices of $P(s)$ and $K(s)$ are given by
Plant $P(s)$:

$$\begin{aligned} A_p &= \begin{bmatrix} -0.1 & 0 \\ 0 & -0.1 \end{bmatrix}, B_p = \begin{bmatrix} 0.5 & 0.4 \\ 0.4 & 0.3 \end{bmatrix} \\ C_p &= \begin{bmatrix} 1 & 0 \\ 0 & 1 \end{bmatrix} \end{aligned}$$

Controller $K(s)$:

$$\begin{aligned} A &= \begin{bmatrix} 0 & 0 \\ 0 & 0 \end{bmatrix}, B = \begin{bmatrix} 1 & 0 \\ 0 & -1 \end{bmatrix} \\ C &= \begin{bmatrix} 1 & 0 \\ 0 & 1 \end{bmatrix}, D = \begin{bmatrix} 10 & 0 \\ 0 & -10 \end{bmatrix} \end{aligned}$$

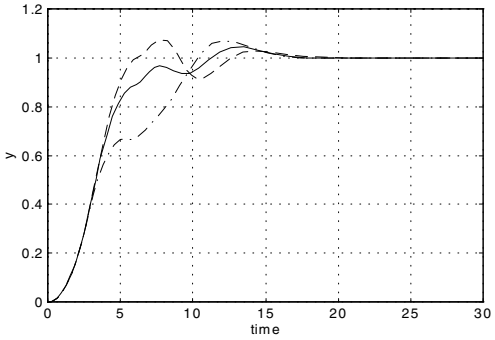

Fig. 12. $y(t)$ (dashed:$\epsilon = 0.7$, solid:$\epsilon = 1.2$, dash-dot:$\epsilon = 5$)

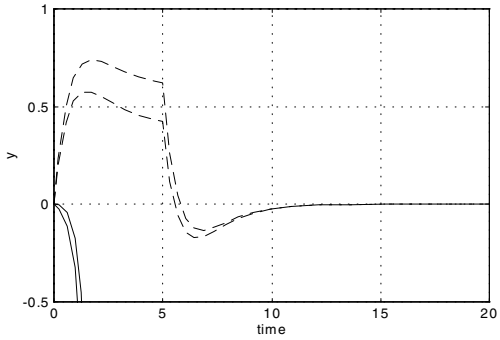

Fig. 14. $y(t)$ (solid:constrained w/o AWC, dashed:unconstrained)

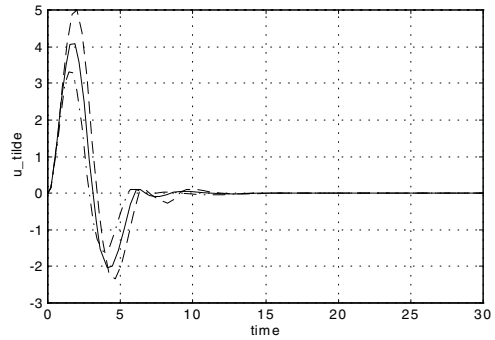

Fig. 13. $\tilde{u}(t)$ (dashed:$\epsilon = 0.7$, solid:$\epsilon = 1.2$, dash-dot:$\epsilon = 5$)

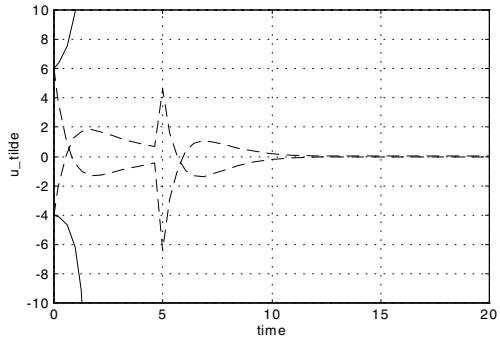

Fig. 15. $\tilde{u}(t)$ (solid:constrained w/o AWC, dashed:unconstrained)

The limitations on controller outputs are $|u_1| \leq 3$ and $|u_2| \leq 10$.

We solved Problem 1 with $\epsilon = 4.5, \bar{\kappa} = \text{diag}[1, 1]$, and obtained a feasible solution

$$H = \begin{bmatrix} 3.3964 & 0.7548 \\ -2.7222 & -0.3392 \end{bmatrix}$$

Note that the closed-loop system is globally stabilized by using this anti-windup compensator, since this compensator is obtained for $\bar{\kappa} = \text{diag}[1, 1]$.

Next, we will show some results of numerical simulations for the step reference command given by

$$r(t) = \begin{cases} (0.6, 0.4)^T, & (0 \leq t \leq 5) \\ (0, 0)^T, & (5 < t) \end{cases}$$

Fig.14 and Fig.15 show the responses of the constrained system (solid) and the unconstrained system (dashed). The input saturations destroy the closed-loop stability in this case. Fig.16 and Fig.17 show the responses of the system with the anti-windup compensator designed by the Conditioning Technique (CT) [4]. In this numerical example, CT fails to stabilize the closed-loop system. Fig.18 and Fig.19 show the responses of the system with the proposed anti-windup compensator. Although it takes long time to reach the reference values, the closed-loop stability is assured by using the proposed anti-windup compensator.

C. Example 3 (Control of a BTT Missile)

In this section, we consider a control problem of a Bank-to-Turn (BTT) missile with saturating actuators [16]. The linearized model of the yaw/roll dynamics of the BTT missile is described by

$$\begin{aligned} A_p &= \begin{bmatrix} -0.818 & -0.999 & 0.349 \\ 80.29 & -0.579 & 0.009 \\ -2734 & 0.5621 & -2.10 \end{bmatrix} \\ B_p &= \begin{bmatrix} 0.147 & 0.012 \\ -194.4 & 37.61 \\ -2176 & -1093 \end{bmatrix} \\ C_p &= \begin{bmatrix} 1 & 0 & 0 \\ 0 & 1 & 0 \end{bmatrix} \end{aligned}$$

The nominal controller $K(s)$ designed by the LQG/LTR design methodology has a state space representation given by

$$A = \begin{bmatrix} A_1 & B_1 \\ 0 & 0 \end{bmatrix}, B = \begin{bmatrix} 0 \\ I \end{bmatrix}, D = \begin{bmatrix} C_1 & 0 \end{bmatrix}$$

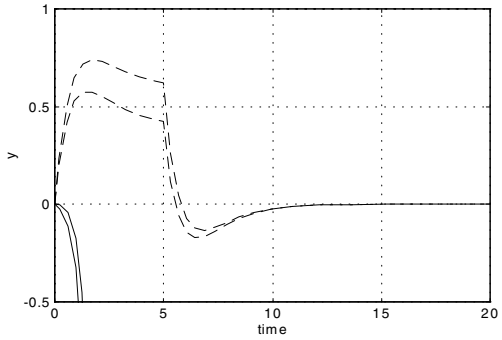

Fig. 16. $y(t)$ (solid:CT [4], dashed:unconstrained)

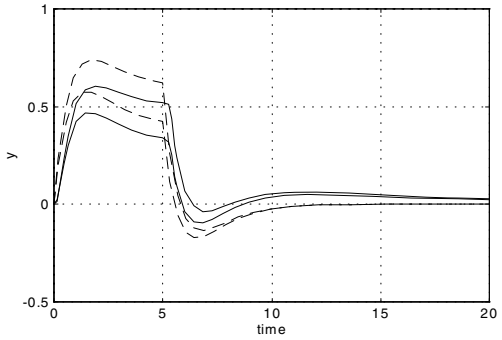

Fig. 18. $y(t)$ (solid:with proposed AWC, dashed:unconstrained)

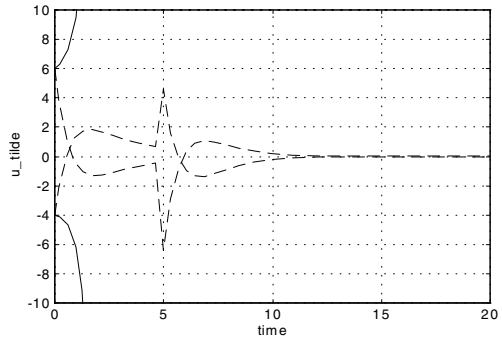

Fig. 17. $\tilde{u}(t)$ (solid:CT [4], dashed:unconstrained)

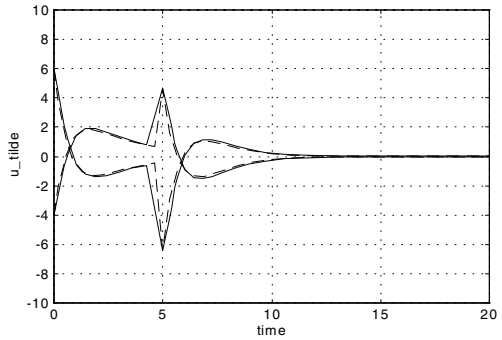

Fig. 19. $\tilde{u}(t)$ (solid:with proposed AWC, dashed:unconstrained)

where

$$A_1 = \begin{bmatrix} -0.29 & -107.78 & 6.67 & -2.58 & -0.40 \\ 107.68 & -97.81 & 63.95 & -4.52 & -5.35 \\ -6.72 & 64.82 & -54.19 & -40.79 & 5.11 \\ 3.21 & 2.10 & 29.56 & -631.15 & 429.89 \\ 0.36 & -3.39 & 3.09 & -460.03 & -0.74 \end{bmatrix}$$

$$B_1 = \begin{bmatrix} 2.28 & 0.48 \\ -40.75 & 2.13 \\ 18.47 & -0.22 \\ -2.07 & -44.68 \\ -0.98 & -1.18 \end{bmatrix}$$

$$C_1 = \begin{bmatrix} 0.86 & 8.54 & -1.71 & 43.91 & 1.12 \\ 2.17 & 39.91 & -18.39 & -8.51 & 1.03 \end{bmatrix}$$

Both controller outputs are constrained between the saturation limits ± 8. We solved Problem 1 with $\epsilon = 1, \bar{\kappa} = \text{diag}[1, 1]$, and obtained a feasible solution

$$H = \begin{bmatrix} -0.426 & -2.157 \\ -0.375 & -0.721 \\ -0.631 & 1.273 \\ -7.503 & -3.715 \\ -9.972 & 1.695 \\ -0.079 & -0.987 \\ -0.733 & 0.123 \end{bmatrix}$$

Note that the closed-loop system is globally stabilized by using the obtained anti-windup compensator, since this compensator is obtained for $\bar{\kappa} = \text{diag}[1, 1]$.

Fig.20 and Fig.21 show the responses of the system for $r(t) = [4.2, -4.2]^T, (t \geq 0)$. Although the constrained system without the anti-windup compensator becomes unstable (dashed), the closed-loop stability is assured by using the proposed anti-windup compensator (solid).

In Fig.22 and Fig.23, dashed lines show the responses of the system with the anti-windup compensator designed by the method of Watanabe *et. al* [5] and dash-dot lines show the responses of the system with GCT [15]. The responses of the system with [5] show good performance and GCT fails to stabilize the closed-loop system in this example.

Fig.24 and Fig.25 show the responses of the system in the case where both inputs are constrained between ± 1. In this case, the responses of the system with the proposed anti-windup compensator (solid) are faster than those of the system with the compensator design by [5].

V. Conclusion

We have proposed a design method of a static anti-windup compensator which guarantees robust stability of the closed-loop system.

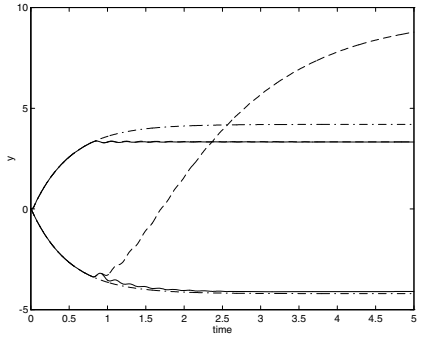

Fig. 20. $y(t)$ (solid:with proposed AWC, dashed:constrained w/o AWC, dash-dot:unconstrained)

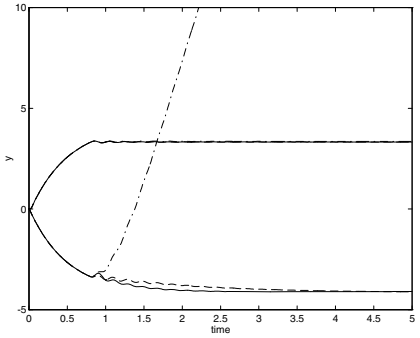

Fig. 22. $y(t)$ (solid:with proposed AWC, dashed:Watanabe *et al.*[5], dash-dot:GCT[15])

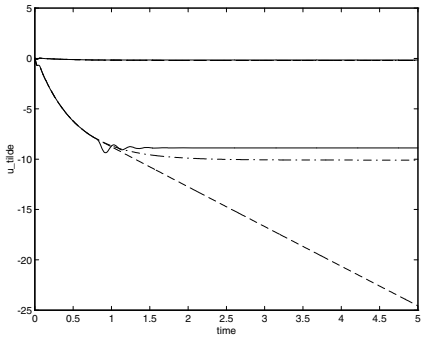

Fig. 21. $\tilde{u}(t)$ (solid:with proposed AWC, dashed:constrained w/o AWC, dash-dot:unconstrained)

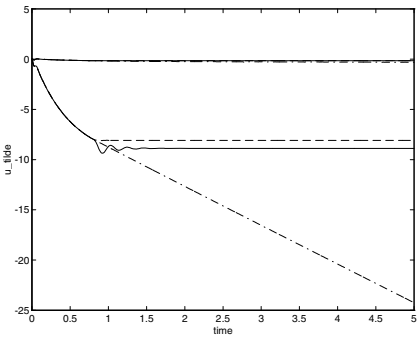

Fig. 23. $\tilde{u}(t)$ (solid:with proposed AWC, dashed:Watanabe *et al.* [5], dash-dot:GCT[15])

- It has been shown that the design problem of a static anti-windup compensator which guarantees closed-loop stability can be reduced to an equivalent LMI problem and can be solved efficiently by using a numerical optimization algorithm. This result is remarkable, since this design problem has been considered a BMI problem.
- In numerical examples 2 and 3, it has been shown that the proposed anti-windup compensator can guarantee global asymptotic stability of the closed-loop system. Although such a solution can not be always obtained, it has been shown in numerical example 1 that the proposed anti-windup compensator can expand the region of attraction effectively.
- The proposed design method is applicable to any control system with an LTI controller. Further, we can put any structural constraint on H. Thus we can design a decentralized anti-windup compensator for a decentralized controller by choosing a block-diagonal matrix as H.

REFERENCES

[1] M.V.Kothare, P.J.Campo, M.Morari,and C.N.Nett: A Unified Framework for the Study of Anti-Windup Designs; *Automatica*, Vol.30, No.12, pp.1869-1883, 1994

[2] M.V.Kothare and M.Morari: Multivariable Anti-Windup Controller Synthesis using Multi-Objective Optimization; *Proc. of American Contr. Conf.*, pp.3093-3097, 1997

[3] V.R.Marcopoli and S.M.Phillips: Analysis and synthesis tools for a class of actuator-limited multivariable control systems: A linear matrix inequality approach; *International Journal of Robust and Nonlinear control*, Vol.6, pp.1045-1063, 1996

[4] R.Hanus, M.Kinnaert and J.L.Henrotte: Conditioning Technique, a General Anti-windup and Bumpless Transfer Method; *Automatica*, Vol.23, No.6, pp.729-739, 1987

[5] R.Watanabe, A.Matui and K.Uchida: Design and Implementation of Anti-Windup Controller Based on State Feedback H^∞ Control Theory; *Proc. of IEE of Japan*, Vol.117-C, No.3, pp.307-314, 1997 (in Japanese)

[6] M.Saeki and N.Wada: Anti-Windup controller design based on Matrix Inequalities; *Proc. of 35th IEEE Conf. on Decision & Control*, pp.261-262, 1996

[7] N.Wada and M.Saeki: Robust controller design for the system with input saturation, *Proc. of 21st SICE Symposium on Dynamical System Theory*, pp.221/226, 1998 (in Japanese)

[8] P.J.Campo and M.Morari: Robust Control of Process subject to Saturation Nonlinearities; *Computers & Chemical Engineering*,Vol.14, No.4/5, pp.343-358, 1990

[9] S.Boyd, L.E.Ghaoui, E.Feron and V.Balakrishman: *Linear Matrix Inequalities in System and Control Theory*, SIAM, 1994

[10] K.C.Goh, M.G.Safonov and G.P.Papavassilopoulos: A Global Optimization Approach for the BMI Problem; *Proc. of 33rd IEEE Conf. on Decision & Control*, pp.2009-2014, 1994

[11] H.H.Rosenbrock: *Multivariable Circle Theorems, Recent Math. De-*

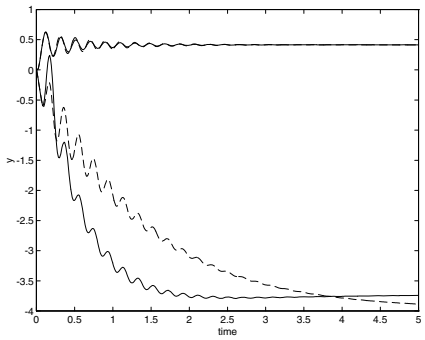

Fig. 24. $y(t)$ (solid:with proposed AWC, dashed:Watanabe *et al.*[5])

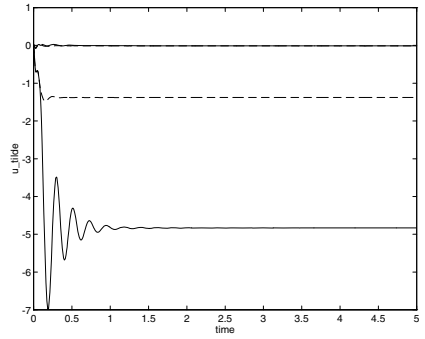

Fig. 25. $\tilde{u}(t)$ (solid:with proposed AWC, dashed:Watanabe *et al.*[5])

velopments in Control; edited by D.J.Bell, Academic Press, London, pp.345-365, 1973

[12] P.Gahinet, A.Nemirovski, A.J.Laub and M.Chilali: *LMI Control Toolbox*; The Math Works Inc., 1995

[13] N.Suda et al.: *PID Control*, Asakura Publishing Co.,Ltd., pp.51-52, 1992

[14] A.H.Glattfelder and W.Schaufelberger: Start-up performance of different proportional-integral-anti-wind-up regulators; *International Journal of Control*, Vol.44, No.2, pp.493-505, 1986

[15] K.S.Walgama and J.Sternby: Inherent observer property in a class of anti-windup compensators; *International Journal of Control*, Vol.52, No.3, pp.705-724, 1990

[16] A.A.Rodriguez and J.R.Cloutier: Control of Bank-to-Turn (BTT) Missile with Saturating Actuators; *Proc. of American Contr. Conf.*, pp.1660-1664, 1994